Microchimica Acta (2022) 189: 104
https://doi.org/10.1007/s00604-022-05211-x

ORIGINAL PAPER

A colorimetric sensor for *Staphylococcus aureus* detection based on controlled click chemical-induced aggregation of gold nanoparticles and immunomagnetic separation

Yushen Liu[1,2,3] · Xuechen Wang[2] · Xuening Shi[2] · Mengyue Sun[1] · Luliang Wang[1,3] · Zhenhua Hu[1,3] · Fangjie Liu[1,3] · Quanwen Liu[1] · Ping Wang[1,3] · Juan Li[2] · Chao Zhao[2]

Received: 14 November 2021 / Accepted: 30 January 2022 / Published online: 14 February 2022
© The Author(s), under exclusive licence to Springer-Verlag GmbH Austria, part of Springer Nature 2022

Abstract

Staphylococcus aureus (*S. aureus*) is a pathogen closely associated with foodborne diseases. We prepared a reliable colorimetric sensor to detect *S. aureus* using click chemical reaction and immunomagnetic separation. Aptamer-functionalized and ALP-labeled Fe_3O_4 NPs act as separation and signal transduction elements. Under the optimized conditions, the Cu^+ generated by signal transduction triggers a click chemistry reaction, which causes the aggregation of azides and alkyne-AuNPs and a color change. The net extinction ratio of $\Delta(A_{530}/A_{760})$ was linearly correlated with the *S. aureus* concentration from 10 to 10^6 cfu mL^{-1}, and the limit detection was 2.4 cfu mL^{-1}. The recoveries were 91.15 ~ 106.36% for the analysis of spiked food and water samples without pre-enrichment. Therefore, we believe that the detection platform can be easily and accurately used for *S. aureus* detection, providing a broad prospect for on-site visual detection.

Keywords *Staphylococcus aureus* · Click chemistry · Aptamer · Colorimetric detection · One-step detection

Introduction

Food safety issues caused by foodborne pathogens have become the focus of public health concerns all over the world [1]. As a highly pathogenic food-borne pathogenic bacterium, *Staphylococcus aureus* (*S. aureus*) can cause acute food poisoning [2]. Quickly and accurately identifying the pathogens throughout the food supply chain is a way to prevent and control foodborne disease outbreaks. Classical pathogen detection methods mainly include plate counting, enzyme-linked immune-sorbent assay (ELISA), polymerase chain reaction (PCR), and loop-mediated isothermal amplification (LAMP) [3–5]. However, they are restricted by time-consuming, labor-intensive, high detection limit, low automation, and complex sample pretreatment [6, 7].

In recent years, the emergence of nanotechnology opens the new horizon to overcome above obstacles. Some researchers have developed new bacterial isolation methods using magnetic beads (MB) to achieve the rapid isolation of target bacteria [8, 9]. It solves the problems of complex substrate and low bacterial concentration of food samples and realizes fast separation and efficient capture of target bacteria. Gold nanoparticles (Au NPs) have been favored by colorimetric researchers in recent years owing to their excellent chemical properties of size controlling, high biocompatibility, and long-term stability [10, 11]. However, the AuNPs-based colorimetric assay is usually susceptible to interference from ambient conditions (i.e., pH value, ion concentration, and temperature), thus affecting the sensitivity of bacterial detection [12, 13]. Copper (I) ions (Cu^+) catalyzed click chemistry (alkyne-azide cycloaddition) can be selectively catalyzed by trace amount of Cu^+, which provides a new way to improve the sensitivity of detection system. Therefore, due to the excellent properties of gold nanoparticles, the "click chemistry" reaction based on gold nanoparticles has attracted wide attention in recent years

✉ Yushen Liu
yushenlys@163.com

✉ Chao Zhao
czhao0529@jlu.edu.cn

[1] College of Food Engineering, Ludong University, Yantai 264025, Shandong, China

[2] School of Public Health, Jilin University, Changchun 130021, China

[3] Bio-Nanotechnology Research Institute, Ludong University, Yantai 264025, Shandong, China

[14, 15]. In the presence of Cu^{+}, a click reaction occurs between azide- and alkyne-functionalized AuNPs, resulting in the aggregation of nanoparticles and the color of the solution changing from red to blue [16]. In addition, Cu^{+} sources can be easily and inexpensively generated to reduce Cu^{2+} by ascorbic acid. Due to their high efficiency and selectivity, "click chemistry" has attracted more and more attention in colorimetric reactions [17, 18].

Inspired by this, we propose a colorimetric strategy based on the click chemistry indicator of AuNPs functionalized with alkyne and azide functional groups (alkyne and azide—AuNPs). In proposed method, the aptamer and ALP dual-labeled Fe_3O_4 NPs (IMB) serve as recognition and signal transduction element. The exogenous L-ascorbate-2-phosphate (AP) was first captured by ALP and then catalyzed to form to ascorbic acid (AA). Then, the Cu^{2+} in the solution was reduced to Cu^{+} by AA. The produced Cu^{+} triggered a click chemical reaction, causing color change recognized by the naked eyes. The binding of IMB to the bacterial surface prevents the substrate from entering the catalytically active site [19], inhibiting the colorimetric sensing of bacteria, which correlates with the concentration of *S. aureus*. Therefore, a colorimetric detection strategy with high sensitivity and specificity is proposed to quantify *S. aureus*.

Experimental section

Materials and reagents

Ferric chloride ($FeCl_3{\cdot}6H_2O$), sodium citrate, and ethylene glycol were purchased from Tianjin Chemical Reagent Co., Ltd. (Tianjin, China) (http://5497614.1024sj.com). Chloroauric acid ($HAuCl_4{\cdot}3H_2O$) was obtained from Aladdin Reagents Co., Ltd. (Shanghai, China) (https://www.aladdin-e.com/). $CuSO_4$ and methanol were received from Beijing Chemical Reagent Co., Ltd. (Beijing, China) (http://www.crc-bj.com). N_3-PEG-SH and CH-PEG-SH were purchased from Ponsure Company (Shanghai, China) (http://www.ponsure.com/). Poly(ethylene glycol) (PEG 6000), alkaline phosphatase (ALP), 2-phospho-L-ascorbic acid trisodium salt (> 95%, HPLC, AP), N-(3-(dimethylamino)-propyl)-N′-ethylcarbodiimide hydrochloride (EDC HCl), and N-hydroxysuccinimide (NHS) were bought from Sigma-Aldrich (http://www.sigmaaldrich.com). 5′-Amine-modified DNA aptamer (5′NH_2—GCA ATG GTA CGG TAC TTC CTC GGC ACG TTC TCA GTA GCG CTC GCT GGT CAT CCC ACA GCT ACG TCA AAA GTG CAC GCT ACT TTG CTA A -3′) was selected according to literature [20] to identify *S. aureus*, which was synthesized by Sangon Biotech Co., Ltd. (Shanghai, China) (http://www.sangon.com). All other chemicals and reagents used were of analytical grade.

All the UV–Vis absorption spectra were collected using a TU-1810 DPC (PERSEE, Beijing, China). Transmission electron microscopy (TEM) images were measured on a JEOL JEM-2100F transmission electron microscope (Tokyo, Japan). Magnetic hysteresis loops were measured by a vibrating sample magnetometer (Lake Shore 7410 VSM). Fourier transform infrared spectra (FTIR) from 4000 to 500 cm^{-1} were recorded using a Nicolet 6700 FTIR spectrometer (Thermo Inc., USA). Zeta potential was carried out with a 90 Plus Zeta Nano Brook.

Culture of bacteria

Table S1 in ESM lists the strains used in the experiment. They were all preserved in 15% glycerol at − 80℃. Strains were resuscitated through scribing on Luria–Bertani (LB) agar plates. Each strain was cultivated by the conventional culture method and collected during the exponential growth period. The bacteria concentration was determined by conventional plate counting method. Various concentrations of *S. aureus* in series were obtained by gradient dilution and stored at 4℃ before use.

Synthesis of aptamer-functionalized ALP-labeled Fe_3O_4 NPs (IMB)

We prepared Fe_3O_4-COOH NPs through the previously reported method [21]. Aptamer-functionalized and ALP-labeled Fe_3O_4 NPs (IMB) were prepared with slight modification according to the method recorded in the literature [22]. Firstly, EDC and NHS (10 mg) were added to activate Fe_3O_4-COOH NPs (0.5 mg) for 0.5 h. Then, the mixture was collected by permanent magnet and washed three times with PBS buffer. 0.8 mL PBS buffer containing 1 mg ALP was added to the precipitate and gently rotated for 2 h. Subsequently, 0.1 μm *S. aureus* aptamer was put in and reacted overnight at gentle mixing. After washed with PBS, the IMB was finally suspended in PBS buffer and preserved at 4 ℃.

Synthesis of functionalized AuNPs

Referring to our previous work, the citric acid reduction method was used to synthesize AuNPs [23]. Alkyne- and azide-functionalized AuNPs solutions were prepared according to the literature with little modifications [24]. In brief, a solution of thiol-PEG-N_3 (30 μL, 2 mM in 2:1 methanol/water) was added to the AuNPs solutions (0.5 mL). N_3-PEG-AuNPs were obtained by rotating the mixture at room temperature for 12 h and centrifuging for 20 min. The obtained N_3-PEG-AuNPs were finally re-dispersed in 2:1 methanol/water (0.25 mL). The CH-PEG-AuNPs were obtained by the same method, except that thiol-PEG-CH was replaced with thiol-PEG-N_3. The N_3-PEG-AuNPs and

CH-PEG-AuNPs were mixed to obtain a uniform dispersed solution.

Optimization of experimental conditions

In order to maximize the capture efficiency of *S. aureus*, the concentration of IMB was optimized. *S. aureus* at 10^6 cfu mL^{-1} was taken as an example, and PBS was chosen as the control group. The *S. aureus* suspension were mixed with different concentration of IMB (0.05, 0.1, 0.2, 0.3, 0.4, 0.5, 0.6 mg·mL^{-1}) for 0.5 h. After magnetic separation, the supernatant was spread on LB agar with appropriate dilution for colony count. Based on the plate count method [25], the capture efficiencies of *S. aureus* were obtained.

Our colorimetric method relies on the hydrolysis activity of alkaline phosphatase, so whether the ALP on the IMB surface has the ability to catalyze the hydrolysis of AP is the key point of the colorimetric reaction. According to the previous literature [24, 26], we determined that the detection mixture was composed of N_3-PEG-AuNPs and CH-PEG-AuNPs and Cu^{2+} (1 mM). Based on the optimal amount of IMB, 0.5 mg IMB was incubated with 5 mM AP for 5 min. Then the introduction of detection mixture continued the color reaction. After 5 min, the absorption spectra of 400 to 900 nm were recorded by UV–Vis spectrophotometer.

S. aureus detection assay

Bacteria samples were prepared at different concentrations (10–10^6 cfu mL^{-1}) using sterile PBS and freshly cultured inactivated bacteria. After optimization of experimental conditions, 0.1 mL of each concentration of *S. aureus* solution was incubated with a total of 0.9 mL PBS buffer containing 0.5 mg IMB. At the same time, sterile PBS without bacteria was used as a negative control. The suspension was then slowly shaken in a 1.5-mL plastic centrifuge tube at room temperature for 0.5 h. The solution containing AP (5 mM) was added to each tube after magnetic separation washing. Then, the produced AA was added into the detection mixture (comprising N_3-PEG-AuNPs and CH-PEG-AuNPs and Cu^{2+}). Finally, the absorption spectrum of the solution at 400 ~ 900 nm was recorded with UV–Vis spectrophotometer.

Real sample detection

Spiked water and food samples were used to test the suitability of this colorimetric method. The real samples were prepared according to the literature with little modification [27]. The preparation of pork homogenate was as follows: The pork used in the experiment was bought from the local market. Five grams of samples and 10 mL sterilized PBS were ground until homogenized. The collected lake water samples and pork homogenate were filtered through a 0.22-μm filter. We used the filtrate as a solution instead of PBS buffer to simulate the real sample detection. The filtrate was inoculated with *S. aureus* at different concentrations to prepare the real sample standard. The procedure was identical to the steps described in the part of *S. aureus* analysis, similarly, with food filtrate used as a negative control.

Results and discussion

Strategy for S. aureus detection

As shown in Fig. 1a, this new visualized biosensor is based on ALP to catalyze the hydrolysis of AP to form ascorbic acid and the reduction product Cu^+ to trigger "click chemistry." The aggregation state of AuNPs changes during signal generation and transduction, and the color of the solution changes from red to blue correspondingly. In the presence of *S. aureus*, due to an antigen–antibody immune response between IMB and *S. aureus*, immune complexes were formed. Immune complexes were collected by magnetic separation and delivered to the reporter probe system. The binding of IMB to the *S. aureus* on surface prevented the substrate from entering the catalytically active site, resulting in a decrease in Cu^+ yield; thus, the color of the detection system gradually changes from blue to red (or purple) with the increase of *S. aureus* concentration, facilitating plasmonic readout with bare eyes (Fig. 1b).

Characterization of IMB and functionalized AuNPs

We performed a series of characterization of the IMB, including TEM, FTIR, zeta potential, and magnetic hysteresis loop. According to the characterization results (please see Supplementary Information), we successfully synthesized spherical IMB with superparamagnetic properties and fast magnetic response, and the prepared IMB has excellent enrichment effect on *S. aureus*.

Alkyne- and azide-functionalized AuNPs were successfully prepared by ligand-exchange reaction. TEM, UV–Vis absorption spectrum, and zeta potential were used to measure and characterize alkyne- and azide-functionalized gold nanoparticles (Fig. S2). These characterization results implied the successful preparation of functionalized AuNPs.

Experimental condition optimization

In order to get the best capture performance of *S. aureus*, various concentrations of IMB were investigated by using *S. aureus* of 10^6 cfu·mL^{-1}. The typical photographs of *S. aureus* colony formation captured by IMB are shown in Fig. S3. Compared with the positive control image in Fig. S3

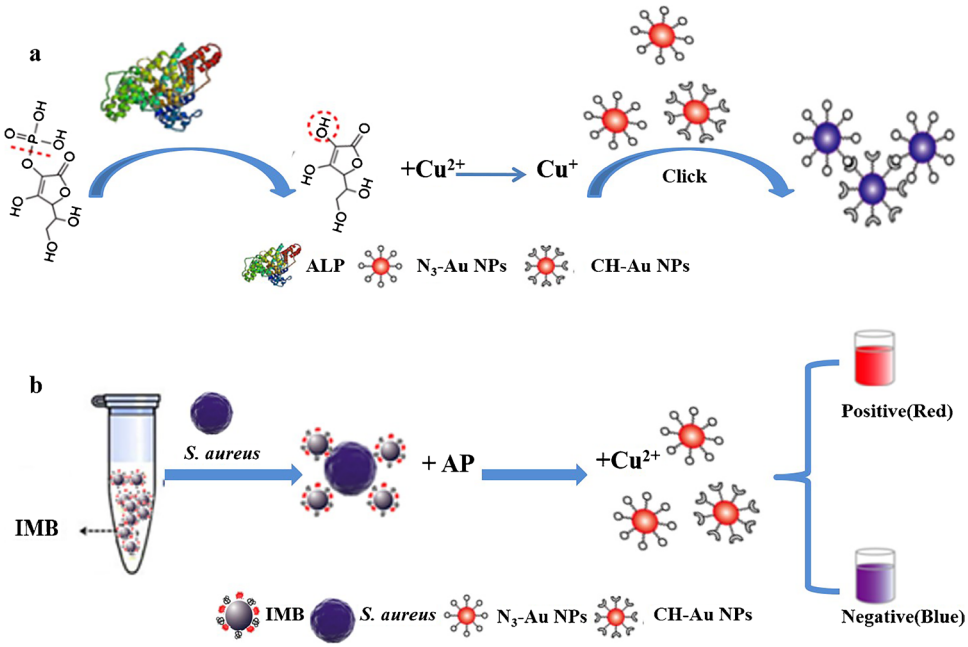

Fig. 1 **a** Cu^{+}-mediated click chemistry response mechanism. **b** Schematic diagram of the proposed colorimetric assay for detection of *S. aureus*

h, the results showed that with the increase of IMB concentration. The number of colonies in enriched supernatant decreased gradually (Fig. S3 a–g). The average colony numbers of *S. aureus* are listed in Table S2. When the concentration was 0.5 mg·mL^{-1}, the capture efficiency was 94.96%, indicating that almost all bacteria were captured by IMB. Further increasing the concentration of IMB, it had weak additional beneficial effects. Hence, follow-up experiments were carried out with 0.5 mg·mL^{-1} IMB.

To verify the ALP activity on the IMB surface, excessive AP was incubated together with IMB. ALP on the surface of IMB hydrolyzes AP to generate AA. The supernatant containing AA reacted with the detection mixture. Cu^{2+} in the detection mixture was reduced by AA to form Cu^{+}, which triggered the click chemistry reaction of functionalized AuNPs, so that the color of the solution changes from red to blue (Fig. 2a), confirming that the ALP activity still existed. The changes in aggregation states of the detection mixture were also observed by the UV–Vis absorption spectra and the TEM images (Fig. 2b, c, d).

Sensitivity detection of S. aureus

To test the sensitivity of the detection system, we conducted experiments on various concentrations of *S. aureus* (10–10^6 cfu·mL^{-1}) under optimum measurement conditions. The photographs in Fig. 3a show that after reacting for 5 min, the detection solution gradually changed from blue to blue-purple, purplish-red, and red with the concentration of *S. aureus* increasing. The naked-eye detection limit of *S. aureus* was determined as 50 cfu·mL^{-1}, which had significant difference from the color of the control sample. The corresponding changes were observed in UV–Vis spectra at the same time (Fig. S4). With the increase of *S. aureus*, the absorption peak gradually increased at 530 nm and decreased at 760 nm, meaning that the aggregation of functionalized AuNPs gradually decreases. We employ the net extinction ratio ($\Delta(A_{530}/A_{760}) = (A_{530}/A_{760})_{Sample}-(A_{530}/A_{760})_{Blank}$) to evaluate the aggregation of the mixture AuNPs solution. $\Delta(A_{530}/A_{760})$ was linearly correlated with the concentration of *S. aureus* at 10–10^6 cfu mL^{-1}. The calibration equation was $\Delta(A_{530}/A_{760}) = 0.137\text{lgC}-0.062$, $R^2 = 0.998$ (Fig. 3b). The detection limit (LOD) for *S. aureus* was calculated as low as 2.4 cfu mL^{-1} (calculated by dividing the standard deviation of the threefold negative control sample by the slope of the fitting standard curve). In order to narrow the influence of large deviations at large concentrations on the regression line, we plotted the linear relationship equation for low concentrations of *S. aureus*. As shown in Fig. 3c, the linear regression equation is $\Delta(A_{530}/A_{760}) = 0.132\text{lgC}-0.050$, $R^2 = 0.992$. Compared with the related reported detection strategies for *S. aureus* (list in Supplementary Material, Table S3), the colorimetric assay we introduced shows excellent performance in terms of detection time, detection steps, and detection limits. This is due to our preparation of a novel dual-labeled magnetic probe modified with ALP and aptamer of *S. aureus*. This dual-labeled nanoprobe has multiple functions of rapid identification, enrichment of target bacteria, and signal transduction. This dual-labeled nanoprobe converted the quantitative signal of *S. aureus*. Through the catalysis of

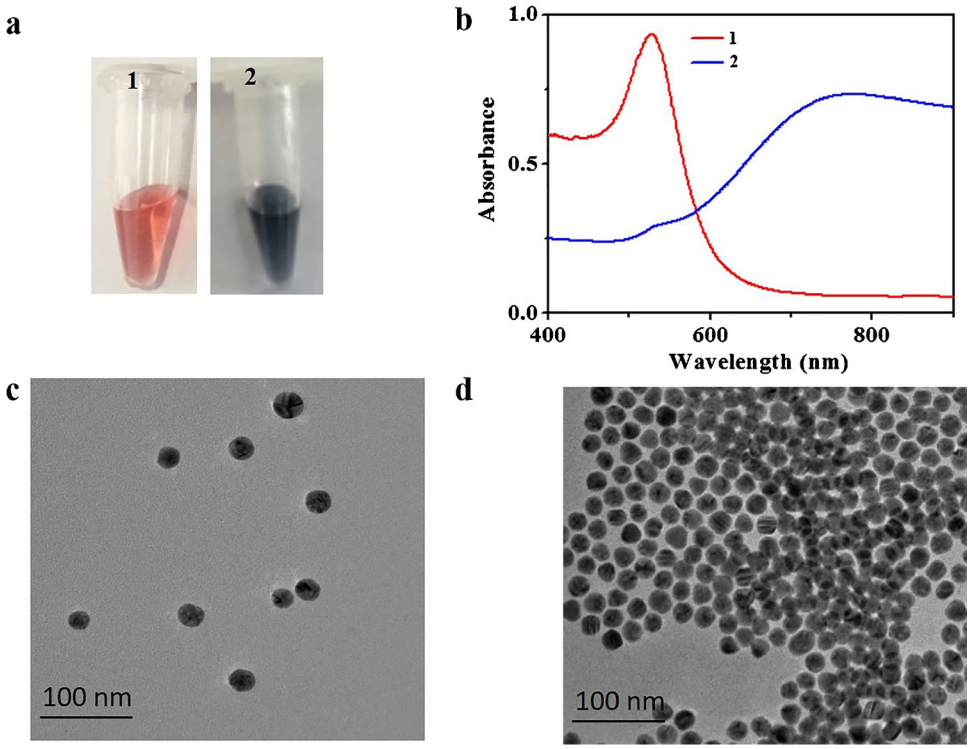

Fig. 2 Photographs (**a**) and UV–Vis spectra (**b**) of experiments to verify ALP activity on IMB surfaces (1, detection mixture; 2, the supernatant of the reaction between IMB and AP + detection mixture). **c** TEM image of the detection mixture. **d** TEM image of the supernatant of the reaction between IMB and AP + detection mixture

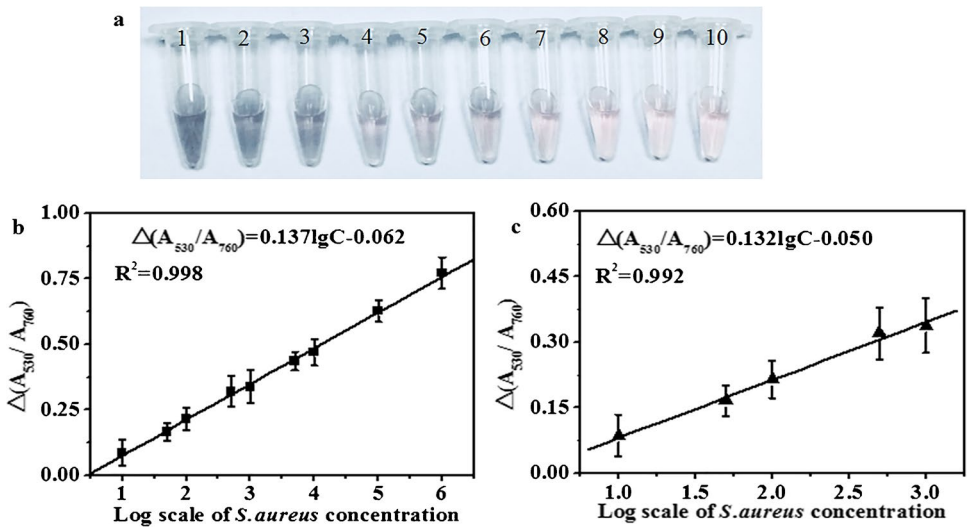

Fig. 3 **a** Photographs of detection system after incubation with different concentrations of *S. aureus*. (1 → 10: 0, 10, 5 × 10, 10^2, 5 × 10^2, 10^3, 5 × 10^3, 10^4, 10^5, and 10^6 cfu·mL^{-1}). **b** The calibration plot for *S. aureus* ($\Delta(A_{530}/A_{760})$ vs. the logarithm of *S. aureus* concentration). **c** The calibration plot for *S. aureus* at 0, 10, 5 × 10, 10^2, 5 × 10^2, and 10^3 cfu·mL^{-1} ($\Delta(A_{530}/A_{760})$ vs. the logarithm of *S. aureus* concentration). Error bars represent the standard deviation of three replicates

ALP and the specific recognition of aptamer, it is converted into the change of Cu^+ concentration in solution. As the carrier of ALP and aptamer, magnetic nanoprobe also takes advantage of its magnetic function to simplify the pretreatment steps. Secondly, we choose alkyne- and azide-functionalized AuNPs as the optical sensors. The click chemistry reaction triggered by Cu^+ led to aggregation of functionalized AuNPs. The state changes of functionalized AuNPs were accompanied by obvious color change, and the semi-quantitative analysis of *S. aureus* can be realized by naked eyes. And our proposed method broadens the application of click chemistry in bacterial detection.

Specificity detection of S. aureus

To evaluate the selectivity of our assay for the target bacteria, the detection system was applied to other interference bacteria, including *E. coli O157:H7*; *V. parahaemolyticus*; *L. monocytogenes*; and *S. typhimurium*, and the absorption spectrum was recorded. Selectivity experiments were performed by identifying *S. aureus* with 10^2 cfu mL^{-1} and interfering bacteria with 10^3 cfu mL^{-1}. The PBS solution was also used as reagent blank. As predicted, all interfering samples and blank samples emerged with a blue color change along with gathered functionalized AuNPs. By contrast, a great color change which transformed from blue to light red was observed, while there is *S. aureus* only and *S. aureus* that coexisted with other interfering bacteria (Fig. 4a). As shown in Fig. 4b, just the existence of *S. aureus* could present a strong absorbance ratio, while the group of interfering substances appeared a bare absorbance ratio. The results showed that 10 folds of other interfering bacteria will not disturb the identification of the target bacteria, demonstrating that the proposed colorimetric assay possessed a good selectivity for *S. aureus*, which can attribute to the synthesized aptamer with high specificity of target bacteria.

Analysis of real samples

To study the application performance of the proposed method in real samples, we selected the spiked lake water and food as the sample model for determination. The proposed method was employed to evaluate different concentrations of *S. aureus* in lake water and pork homogenate. Figure 5 shows the photographs and standard calibration curves of two real samples. Figure 5a and b show the photographs of different concentrations of *S. aureus* in two real sample matrices. The color of the sample tube changes from dark blue, light blue, blue-violet, to red with the increase of *S. aureus*. For the pork matrix, when the concentration is at 10^3 cfu mL^{-1}, there was a clear color difference between the sample and the blank, so the naked-eye readout was 10^3 cfu mL^{-1}, and the naked eye detection limit is 10^2 cfu mL^{-1} in lake water matrix. Because of some impurities in the food matrix, the standard calibration plots of the two real matrix samples were slightly different from those obtained in PBS buffer (Fig. 5c, d). The calibration equation were $\Delta (A_{530}/A_{760}) = 0.1559\text{lgC}-0.0491$, $R^2 = 0.974$ (pork matrix) and $\Delta (A_{530}/A_{760}) = 0.1853\text{lgC}-0.1567$, $R^2 = 0.990$ (lake water matrix). The LOD for *S. aureus* in real samples was calculated to be 9.7 cfu mL^{-1} (pork) and 8.5 cfu mL^{-1} (lake water) (calculated by dividing the standard deviation of the threefold negative control sample by the slope of the fitting standard curve). According to Chinese National Microbiological Criteria, the Australia/New Zealand Standard Methods for Food Microbiology and Microbiological Criteria for Food Stuffs of the European Communities, the coagulase-positive Staphylococci limits for meat and tap water were 100 CFU/g and 100 CFU/mL, respectively [28]. This means that the proposed method could be sufficient to detect *S. aureus* in real world. As described in Table 1, the spiked samples in low concentration (5.0×10 cfu mL^{-1}), medium concentration (5.0×10^2 cfu mL^{-1}), and high concentration (5.0×10^3 cfu mL^{-1}) were measured. The results showed that the average recovery rate was 91.15–106.36%, and the relative standard deviations (RSD) ranged from 7.30 to 13.87%, which proves that the method has good stability and consistency. Meanwhile, it should be noted that the color of all sample's solution can be distinguished by the naked eye (Fig. S5). Thus, the colorimetric assay we proposed can easily realize the one-step detection and examination of *S. aureus* in real samples.

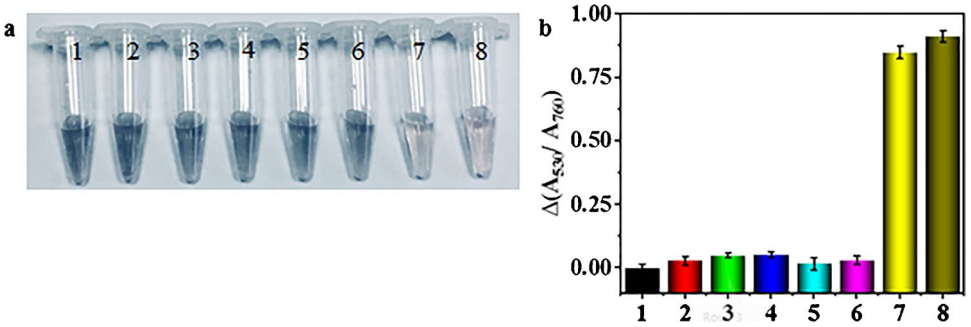

Fig. 4 Selectivity test between the target bacteria *S. aureus* and potential interferences. The concentration of *S. aureus* was 10^2 cfu mL^{-1}, and that of other bacteria was 10^3 cfu mL^{-1}. **a** Photographs of the proposed colorimetric assay in the presence of different analytes (1 → 8: blank, *V. parahaemolyticus*, *E. coli O157:H7*, *L. monocytogenes*, *S. typhimurium*, mixture, *S. aureus* + mixture, and *S. aureus*). **b** The ratio of $\Delta(A_{530}/A_{760})$ of the AuNPs in response to different analytes. Error bars represent the standard deviation of three replicates

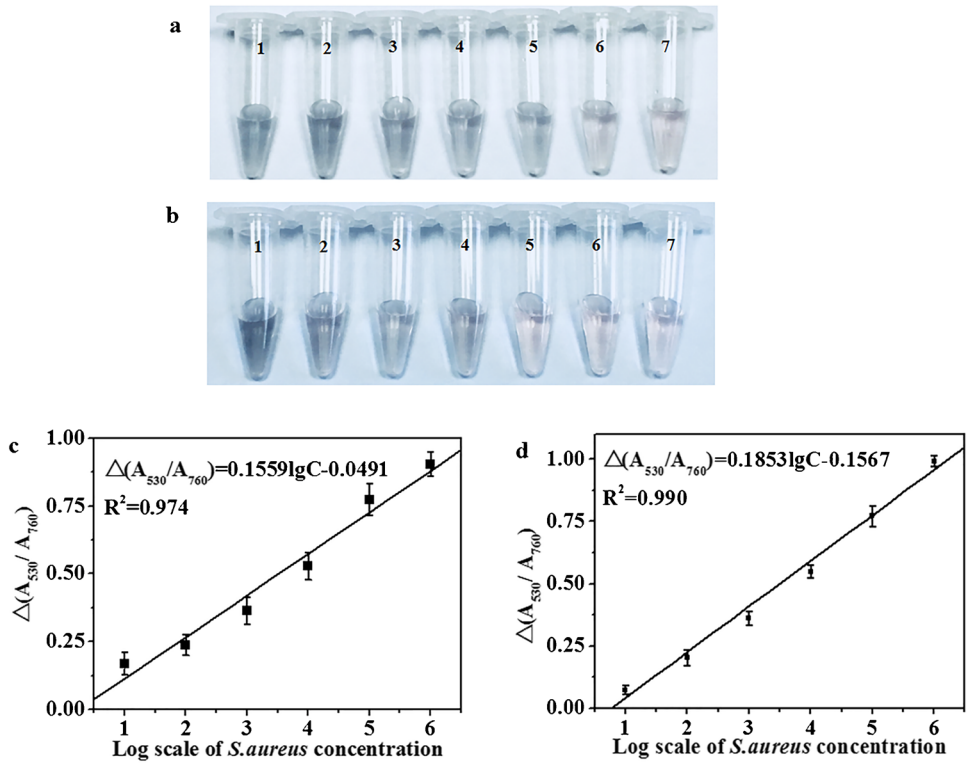

Fig. 5 Detect *S. aureus* in real samples. Photographs of detection system after incubation with different concentrations of *S. aureus* in pork (**a**) and lake water matrix (**b**) (1 → 7: 0, 10, 10^2, 10^3, 10^4, 10^5, and 10^6 cfu·mL^{-1}). The standard calibration plots of the pork (**c**) and lake water matrix (**d**)

The analytical performance and detection effect of the sensor for *S. aureus* were investigated comprehensively, and the results are basically satisfactory. However, the proposed method still has some limitations. One of the biggest defects was that our materials cannot be reused. Although the cost of material synthesis was very low, there were still cumbersome shortcomings in the synthesis process. Secondly, our proposed method largely depends on the catalysis of ALP. Although ALP has specificity and high catalytic activity, as a natural enzyme, it will also be affected by external factors and reduce its stability. Therefore, if this sensor is to be applied to a wider range of fields, it must be committed to developing reusable probes to further improve the detection activity.

Conclusion

A reliable colorimetric method with high sensitivity and good selectivity for the detection of *S. aureus* in food was established. Our proposed approach has the following highlights: (1) the aptamer and ALP dual-labeled magnetic nanoparticles could not only capture *S. aureus* but also hydrolyze AP to induce "click chemistry." Benefit from its excellent enrichment efficiency and high enzyme catalytic activity, the analysis can be completed within 1 h. (2) The click chemistry reaction induced the aggregation of functionalized AuNPs accompanied by a visible color change from blue to red. The concentration of bacteria can be judged semi-quantitatively by color change. At the same time, the

Table 1 The recoveries and RSD values of detecting bacteria in spiked pork samples ($n = 3$)

Sample	Found (cfu mL^{-1})	Added (cfu mL^{-1})	Calculated (cfu mL^{-1})	Recovery rate (%)	RSD (%)
Lake water	BDL[a]	5×10	$(5.31\pm0.55)\times10$	106.36	10.32
	BDL	5×10^2	$(4.58\pm0.44)\times10^2$	91.15	9.61
	BDL	5×10^3	$(4.83\pm0.35)\times10^3$	96.56	7.30
Pork	BDL	5×10	$(4.80\pm0.60)\times10$	95.98	12.41
	BDL	5×10^2	$(4.92\pm0.68)\times10^2$	98.43	13.87
	BDL	5×10^3	$(4.75\pm0.48)\times10^3$	95.90	10.08

[a]*BDL* below detection limit

proposed method broadens the application of click chemistry reaction in bacterial detection. (3) The application of multifunctional nanoprobes makes the method less demanding and easy to operate. These advantages make us believe that the colorimetric method developed by us has great application potential in monitoring *S. aureus* and on-site detection.

Supplementary Information The online version contains supplementary material available at https://doi.org/10.1007/s00604-022-05211-x.

Funding This study was supported by the Chinese National Natural Science Foundation (Grant Nos. 82003502, 82073557, 81872668, and 21904053).

Declarations

Conflict of interest The authors declare no competing interests.

References

1. Yin M, Jing C, Li H, Deng Q, Wang S (2020) Surface chemistry modified upconversion nanoparticles as fluorescent sensor array for discrimination of foodborne pathogenic bacteria. J Nanobiotechnol 18:41–54. https://doi.org/10.1186/s12951-020-00596-4
2. Shahdordizadeh M, Taghdisi SM, Ansari N, AlebooyeLangroodi F, Abnous K, Ramezani M (2017) Aptamer based biosensors for detection of Staphylococcus aureus. Sensors Actuators B Chem 241:619–635. https://doi.org/10.1016/j.snb.2016.10.088
3. Teng J, Yuan F, Ye Y, Zheng L, Yao L, Xue F, Chen W, Li B (2016) Aptamer-based technologies in foodborne pathogen detection. Front Microbiol 7:1426–1436. https://doi.org/10.3389/fmicb.2016.01426
4. Zhou B, Chen B, Wu X, Li F, Yu P, Aguilar ZP, Wei H, Xu H (2016) A new application of a sodium deoxycholate-propidium monoazide-quantitative PCR assay for rapid and sensitive detection of viable Cronobacter sakazakii in powdered infant formula. J Dairy Sci 99:9550–9559. https://doi.org/10.3168/jds.2016-11538
5. Pang B, Ding X, Wang G, Zhao C, Xu Y, Fu K, Sun J, Song X, Wu W, Liu Y, Song Q, Hu J, Li J, Mu Y (2017) Rapid and quantitative detection of vibrio parahemolyticus by the mixed-dye-based loop-mediated isothermal amplification assay on a self-priming compartmentalization microfluidic chip. 65(11312–11319):11312–11319. https://doi.org/10.1021/acs.jafc.7b03655
6. Yuan J, Wu S, Duan N, Ma X, Xia Y, Chen J, Ding Z, Wang Z (2014) A sensitive gold nanoparticle-based colorimetric aptasensor for Staphylococcus aureus. Talanta 127:163–168. https://doi.org/10.1016/j.talanta.2014.04.013
7. Niemz A, Ferguson TM, Boyle DS (2011) Point-of-care nucleic acid testing for infectious diseases. Trends Biotechnol 29:240–250. https://doi.org/10.1016/j.tibtech.2011.01.007
8. Bezdekova J, Zemankova K, Hutarova J, Kociova S, Smerkova K, Adam V, Vaculovicova M (2020) Magnetic molecularly imprinted polymers used for selective isolation and detection of Staphylococcus aureus. Food Chem 321:126673–126680. https://doi.org/10.1016/j.foodchem.2020.126673
9. Jung SH, Hahn YK, Oh S, Kwon S, Um E, Choi S, Kang JH (2018) Advection flows-enhanced magnetic separation for high-throughput bacteria separation from undiluted whole blood. Small 14:1801731–1801737. https://doi.org/10.1002/smll.201801731
10. Liu Y, Wang J, Song X, Xu K, Chen H, Zhao C (2018) Colorimetric immunoassay for Listeria monocytogenes by using core gold nanoparticles, silver nanoclusters as oxidase mimetics, and aptamer-conjugated magnetic nanoparticles. Microchim Acta 185:360–366. https://doi.org/10.1007/s00604-018-2896-1
11. Fu K, Zheng Y, Li J, Liu Y, Pang B, Song X, Xu K, Wang J, Zhao C (2018) Colorimetric immunoassay for rapid detection of vibrio parahemolyticus based on Mn(2+) mediates the assembly of gold nanoparticles. J Agric Food Chem 66:9516–9521. https://doi.org/10.1021/acs.jafc.8b02494
12. Amini A, Kamali M, Amini B, Najafi A, Narmani A, Hasani L, Rashidiani J, Kooshki H, Elahi N (2019) Bio-barcode technology for detection of Staphylococcus aureus protein A based on gold and iron nanoparticles. Int J Biol Macromol 124:1256–1263. https://doi.org/10.1016/j.ijbiomac.2018.11.123
13. You Q, Zhang X, Wu F-G, Chen Y (2019) Colorimetric and test stripe-based assay of bacteria by using vancomycin-modified gold nanoparticles. Sens Actuators B Chem 281:408–414. https://doi.org/10.1016/j.snb.2018.10.103
14. Mou X-Z, Chen X-Y, Wang J, Zhang Z, Yang Y, Shou Z-X, Tu Y-X, Du X, Wu C, Zhao Y, Qiu L, Jiang P, Chen C, Huang D-S, Li Y-Q (2019) Bacteria-instructed click chemistry between functionalized gold nanoparticles for point-of-care microbial detection. ACS Appl Mater Interfaces 11:23093–23101. https://doi.org/10.1021/acsami.9b09279
15. Zhang XR, Zhang Y, Chen FT, Li Y, Zhang SS (2016) Visual detection of single-nucleotide polymorphisms and DNA methyltransferase based on cation-exchange of CuS nanoparticles and click chemistry of functionalized gold nanoparticles. Chem Commun 52:13261–13264. https://doi.org/10.1039/C6CC06735B
16. Kolb HC, Finn MG, Sharpless KB (2001) Click chemistry: diverse chemical function from a few good reactions. Angewandte Chemie (Int Engl) 40: 2004–2021. https://doi.org/10.1002/1521-3773(20010601)40:11<2004::aid-anie2004>3.3.co;2-5
17. Tarnowska M, Krawczyk T (2020) Click chemistry as a tool in biosensing systems for sensitive copper detection. Biosens Bioelectron 169:112614–112627. https://doi.org/10.1016/j.bios.2020.112614
18. Zhang Z, Li T, Sheng Y, Liu L, Wu H-C (2019) Enhanced sensitivity in nanopore sensing of cancer biomarkers in human blood via click chemistry. Small 15:1804078–1804083. https://doi.org/10.1002/smll.201804078
19. Gong J, Han X, Zhu X, Guan Z (2014) Layer-by-layer assembled multilayer films of exfoliated layered double hydroxide and carboxymethyl-β-cyclodextrin for selective capacitive sensing of acephatemet. Biosens Bioelectron 61:379–385. https://doi.org/10.1016/j.bios.2014.05.044
20. Zhang H, Yao S, Song X, Xu K, Wang J, Li J, Zhao C, Jin M (2021) One-step colorimetric detection of Staphylococcus aureus based on target-induced shielding against the peroxidase mimicking activity of aptamer-functionalized gold-coated iron oxide nanocomposites. Talanta 232:122448–122455. https://doi.org/10.1016/j.talanta.2021.122448
21. Liu Y, Zhao C, Song X, Xu K, Wang J, Li J (2017) Colorimetric immunoassay for rapid detection of Vibrio parahaemolyticus. Microchim Acta 184:4785–4792. https://doi.org/10.1007/s00604-017-2523-6
22. Wu S, Wang Y, Duan N, Ma H, Wang Z (2015) Colorimetric aptasensor based on enzyme for the detection of vibrio parahemolyticus. J Agric Food Chem 63:7849–7854. https://doi.org/10.1021/acs.jafc.5b03224
23. Liu Y, Zhao C, Fu K, Song X, Xu K, Wang J, Li J (2017) Selective turn-on fluorescence detection of Vibrio parahaemolyticus in food based on charge-transfer between CdSe/ZnS quantum dots and gold nanoparticles. Food Control 80:380–387. https://doi.org/10.1016/j.foodcont.2017.05.032

24. Zhou Y, Wang S, Zhang K, Jiang X (2008) Visual detection of copper(II) by azide- and alkyne-functionalized gold nanoparticles using click chemistry. Angew Chem Int Ed 47:7454–7456. https://doi.org/10.1002/anie.200802317
25. Wen C-Y, Jiang Y-Z, Li X-Y, Tang M, Wu L-L, Hu J, Pang D-W, Zeng J-B (2017) Efficient enrichment and analyses of bacteria at ultralow concentration with quick-response magnetic nanospheres. ACS Appl Mater Interfaces 9:9416–9425. https://doi.org/10.1021/acsami.6b16831
26. Qu W, Liu Y, Liu D, Wang Z, Jiang X (2011) Copper-mediated amplification allows readout of immunoassays by the naked eye. Angew Chem Int Ed 50:3442–3445. https://doi.org/10.1002/anie.201006025
27. Zhu S, Tang Y, Shi B, Zou W, Wang X, Wang C, Wu Y (2021) Oligonucleotide-mediated the oxidase-mimicking activity of Mn3O4 nanoparticles as a novel colorimetric aptasensor for ultrasensitive and selective detection of Staphylococcus aureus in food. Sens Actuators B Chem 349:130809–130819. https://doi.org/10.1016/j.snb.2021.130809
28. Lu Y, Yuan Z, Bai J, Lin Q, Deng R, Luo A, Chi Y, Deng S, He Q (2020) Directly profiling intact Staphylococcus aureus in water and foods via enzymatic cleavage aptasensor. Anal Chim Acta 1132:28–35. https://doi.org/10.1016/j.aca.2020.07.058

Publisher's note Springer Nature remains neutral with regard to jurisdictional claims in published maps and institutional affiliations.